

Dear reviewer

Please check our answers point-by-point and manuscripts' changes track.  
Thanks a lot

Jianjun Xu

Response to reviewer#1

General comments

This paper is of interest in that it provides information on the incremental value of assimilating conventional observations and various satellite observations, differentiated by frequency (microwave and infrared). For this reason, I think it is worth publishing once the authors address the following general comments:

The English language used in the text could be improved;

[Answer: Yes, please check we have modified the English writing.](#)

The behaviour of the IASI data assimilation (temperature and humidity) needs further discussion. In particular, I find the discussion in Sect. 5.2 weak;

[Answer: Yes, you are right, because IASI data has 8461 channels, but we only used 279 channels based on previous studies, more experiments are necessary for future study.](#)

Radiance vs retrieval assimilation of satellite data– at the earlier stage of the review I asked a question on whether the assimilation approach in the paper, as I understood it, was fair (retrieval assimilation for conventional data; radiance assimilation for satellite data). As far as I can tell, the authors did not address this question. I think it would be worth at least discussing if the impact of satellite data assimilation would be the same if retrievals rather than radiances were assimilated (as far as I can tell, this is not discussed in the paper). Is any advantage from the satellite data assimilation mainly coming from assimilating radiances or from the spatio-temporal characteristics of the satellite data?

[Answer: As known, in most of weather agencies, such as NOAA, they have already given up retrieval data assimilation. There is a lot of discussion in previous studies, for example: Derber J. C. and W-S Wu. 1998, The use of TOVS cloud-cleared radiances in the NCEP SSI analysis system. \*Mon. Wea. Rev.\*, \*\*126\*\*, 2287–2299.](#)

The main reasons probably come from the following two aspects:

1) The retrieved data error is an extra error for a data assimilation system, the direct radiance data assimilation will avoid the impacts of the potential double error.

2) The retrieval products are generally obtained based on the one dimensional variational approach, in which the model background field has been first used. And then the background field is used again in the process of regional or subsequent data

assimilations to improve the model initialization. It is not reasonable that the background field have been used double time.

The authors should also address the following specific comments.  
Specific comments

P. 6442, L. 20: I suggest you indicate that this often referred to as the NMC method.

Answer: Yes, Please check line 20 on page 5.

P. 6446, L. 7: Uddstrom.

Answer: Done

P. 6446, L. 14: Would it be better to plot histograms of OmA and OmB? Often, this approach is taken in the literature.

Answer: yes, the histograms of OmA and OmB are often plotted in the some literature, but the scatter plot is also good way to directly show the impacts of data assimilation.

P. 6447, L. 15: Why is this interesting? Avoid subjective statements.

Answer : The word 'Interestingly' was removed.

P. 6448, L. 14: What do you mean by "rare" observational data? Do you mean "sparse"?

Answer : Yes. The word "sparse" is better.

P. 6449, L. 11: Fourth.

Answer : Yes.

P. 6458: Fig. 1: I suggest you change the background colour for the land, as the surface pressure locations in the left-hand panel are difficult to see.

Answer: You are probably right. Actually we tried several times using various colors. Because there are many types of datasets used in this study, we found the background color in current plots appeared to be the best color combination.

P. 6461: Fig. 4: Indicate with respect to what dataset is the bias calculated.

Response: Actually we identified the bias calculation, the bias calculation referred to the observations, which is mainly from conventional data.

1 **Impacts of AMSU-A/MHS and IASI Data Assimilation on**  
2 **Temperature and Humidity Forecasts with GSI/WRF**  
3 **over the Western United States**  
4

5 YANSONG BAO

6 Collaborative Innovation Center on Forecast and Evaluation of Meteorological Disasters, Key  
7 Laboratory for Aerosol-Cloud-Precipitation of China Meteorological Administration, Nanjing  
8 University of Information Science and Technology, Nanjing, China  
9 Environmental Science and Technological Center College of Science, George Mason University,  
10 Fairfax, Virginia, USA  
11

12 JIANJUN XU\*

13 Global Environment and Natural Resources Institute  
14 College of Science, George Mason University, Fairfax, Virginia  
15

16 ALFRED M. POWELL, JR.

17 NOAA/NESDIS/STAR, College Park, Maryland  
18

19 MIN SHAO

20 *College of Science, George Mason University*  
21  
22

23  
24 *June-August 1008, 2015*  
25

26 *Revised*

27 **Atmospheric Measurement Techniques**  
28  
29  
30  
31

32 *\*Corresponding author contact information:*

33 **Dr. JIANJUN XU**, Global Environment and Natural Resources Institute (GENRI),  
34 College of Science, George Mason University. Email: [jxu14@gmu.edu](mailto:jxu14@gmu.edu)  
35  
36  
37

1 **Abstract**

2 Using NOAA's Gridpoint Statistical Interpolation (GSI) data assimilation system and  
3 NCAR's Advanced Research WRF (ARW-WRF) regional model, six experiments are designed  
4 by (1) control experiment (CTRL) and five data assimilation (DA) experiments with different  
5 data sets including (2) conventional data only (CON), (3) microwave data (AMSU-A + MHS)  
6 only (MW), (4) infrared data (IASI) only (IR), (5) s combination of microwave and infrared data  
7 (MWIR), and (6) a combination of conventional, microwave and infrared observation data  
8 (ALL). One month experiments in July 2012 and the impacts of the DA on temperature and  
9 moisture forecasts at the surface and four vertical layers, ~~which~~ over the western United States  
10 have been investigated. The four layers include lower troposphere (LT) from 800 to 1000 hPa,  
11 middle troposphere (MT) from 400 to 800 hPa, upper troposphere (UT) from 200 to 400 hPa and  
12 lower stratosphere (LS) from 50 to 200 hPa. The results show that the regional GSI/WRF system  
13 is underestimating the observed temperature in the LT and overestimating in the UT and LS. The  
14 MW DA reduced the forecast bias from the MT to the LS within 30-hour forecasts, and the CON  
15 DA kept a smaller forecast bias in the LT for 2-day forecasts. The largest RMS error is observed  
16 in the LT and at the surface (SFC). Compared to the CTRL, the MW DA made the most positive  
17 contribution in the UT and LS, and the CON DA mainly improved the temperature forecasts at  
18 the SFC. However, the IR DA made a negative contribution in the LT.

19 Most of the observed humidity in the different vertical layers is overestimated in the  
20 humidity forecasts except in the UT. The smallest bias in the humidity forecast occurred at the  
21 SFC and UT. The DA experiments apparently reduced the bias from the LT to UT, especially for  
22 the IR DA experiment, but the RMS errors are not reduced in the humidity forecasts. Compared  
23 to the CTRL, the IR DA experiment has a larger RMS error in the moisture forecast although the

1 smallest bias is found in the LT and MT.

2 Key words: Data assimilation, temperature, humidity, forecast

3

4

5

6

7

8

9

10

11

12

13

14

15

16

17

18

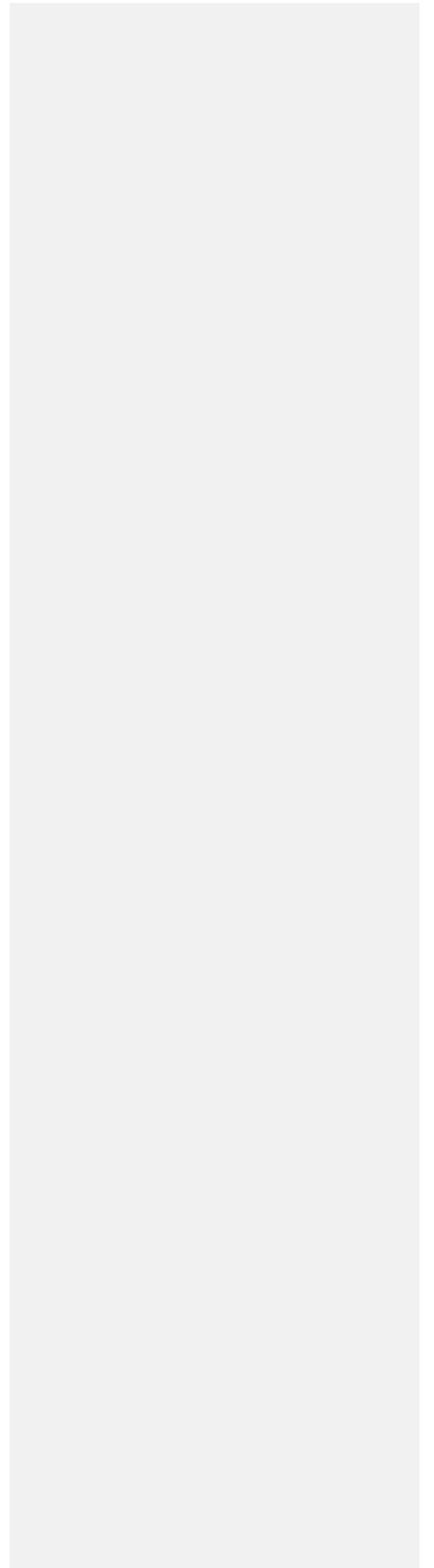
19

20

21

22

23



## 1 1. Introduction

2 Instead of ~~a~~the random distribution and heterogeneous spatial density in the traditional  
3 conventional radiosondes, satellite observations provide a large amount of data covering  
4 worldwide areas for improving the initialization of the weather forecasts models through a data  
5 assimilation system. Many studies demonstrated that the assimilation of satellite data  
6 significantly improved weather forecasts (Eyre 1992; Andersson et al. 1991; Derber and Wu  
7 1998; Zhou et al. 2011), especially over some areas with sparse conventional observations  
8 (McNally et al. 2000; Zapotocny et al. 2008; Liu et al., 2012)

9 The Meteorological Operational satellite program (MetOp) launched its first polar orbiting  
10 satellite (MetOp-A) on October 19, 2006. MetOp-A is in a sun-synchronous orbit, carrying a  
11 payload of 10 scientific instruments including the Advanced Microwave Sounding Unit-A  
12 (AMSU-A), Microwave Humidity Sounder (MHS) and the new generation Infrared Atmospheric  
13 Sounding Interferometer (IASI) to make atmospheric soundings at various altitudes. IASI  
14 (Clerbaux, et al. 2009) measures the radiance emitted from the Earth in 8461 channels covering  
15 the spectral interval  $645\text{-}2760\text{ cm}^{-1}$  at a resolution of  $0.5\text{ cm}^{-1}$  (apodized) and with a spatial  
16 sampling of 18 km at nadir. Limited spectral data is currently transmitted, stored and assimilated.  
17 Rabier et al. (2002) compared a number of techniques for channel selection from high-spectral-  
18 resolution infrared sounders, and concluded that the channel-selection method of Rodgers (1996,  
19 2000) is the ~~most~~-optimal method. Collard (2007) applied his method to select a subset of 300  
20 channels for data assimilation, so that the total loss of information for a typical numerical  
21 weather prediction (NWP) state vector consisting of one or more of temperature, humidity is  
22 minimized.

23 This study focuses on assessing the effects of AMSU-A, MHS and IASI data assimilation

1 on numerical weather forecasts over the western United States. The model, data and  
2 methodology are presented in the section 2 and section 3, respectively. Section 4 describes the  
3 results of experiments. The results are summarized and discussed in section 5.

## 4 **2. Model**

### 5 **2.1 The GSI system for ARW-WRF Regional Model**

6 The assimilation system used here is the Gridpoint Statistical Interpolation (GSI) analysis  
7 system, which is developed by United States National Centers for Environmental Prediction  
8 (NCEP). The current GSI regional analysis system accepts NCEP's Nonhydrostatic Mesoscale  
9 Model (NMM) WRF and NCAR's Advanced Research WRF (ARW) WRF mass core (Liu and  
10 Weng, 2006; Xu and Powell, 2011; Wan and Xu, 2011). ~~The interfaces are~~ specialized  
11 separately for the WRF NMM core and the WRF ARW core. The analysis system produces an  
12 analysis through the minimization of an objective function given by

$$13 \quad J = \frac{1}{2}(x - x^b)^T B^{-1}(x - x^b) + \frac{1}{2}(H(x) - y^o)^T R^{-1}(H(x) - y^o)$$

14 Where  $x$  is the analysis state,  $B$  is the background error covariance matrix,  $x^b$  is the first guess  
15 that ~~is comes~~ from GFS 6-h forecast ~~field led~~ in this study,  $H$  is the transformation operator from  
16 the analysis variable to the form of the observations,  $y^o$  is the observation such as AMSU-A,  
17 MHS, IASI, etc.

18 The minimization algorithm is composed of two outer iterations to account for weak  
19 nonlinearities in the cost function. In the first external iteration the first guess is a 6-h forecast,  
20 while in the second one it is the solution from the previous outer iteration. In the cost function,  
21  $B$  has been estimated from scaled differences between 24-h and 48-h forecasts valid at the same  
22 time (Parrish and Derber, 1992). The observation error covariance matrix ( $R$ ) contains  
23 information on the observational error and errors in representativeness, which has been

1 calculated before running the GSI.

## 2 **2.2 Radiative Transfer Model**

3 The radiative transfer model incorporated into the GSI data assimilation system at the  
4 NCEP is the Community Radiative Transfer Model (CRTM). The CRTM was developed by the  
5 ~~United States~~ Joint Center for Satellite Data Assimilation (JCSDA) for rapid calculations of  
6 satellite radiances based on radiative transfer (RT) theory (Han, et al. 2006). The forward model,  
7 tangent-linear, adjoint and K-matrix models were also developed for ~~the~~ data assimilation of  
8 satellite data. CRTM is always updated for new satellite data. It supports a large number of  
9 sensors onboard geostationary and polar-orbiting satellites, covering the microwave, infrared and  
10 visible frequency regions.

11 The CRTM comprises four major modules: (1) RT solution module, (2) atmospheric  
12 transmittance module, (3) surface emissivity/reflectivity module, (4) particle scattering module.  
13 Six RT solution schemes were tested in the CRTM (Weng et al., 2007). According to several  
14 performance factors, the advance doubling and adding scheme (ADA; Liu and Weng, 2006) was  
15 selected for the CRTM implementation. In CRTM, a fast and optimal spectral sampling (OSS)  
16 absorption model (Moncet et al. 2004) is used to calculate atmospheric transmittance.

## 17 **2.3 Experiment Design**

18 The objective of this study is to explore the effect of satellite data assimilation on the main  
19 atmospheric state forecast ~~throughby~~ -comparing the results from microwave (AMSU-A and  
20 MHS), hyperspectral infrared radiance (IASI) and conventional data assimilation. Over the main  
21 continent of United States of America (USA), there are many conventional observation stations,  
22 which can be used to validate the forecast results. Therefore, the western coast region of the USA  
23 is selected ~~to as~~ the experimental region. ~~Analyzing the satellite data (AMSU-A, MHS and IASI)~~



1 ~~covering the western USA at 00, 06, 12 and 18 UTC, the satellite data at 18 UTC covered more~~  
2 ~~of the region than at other anytime. There were more satellite data coverage of the experimental~~  
3 ~~region around 18 UTC than other time, such as 00, 06, 12 and 18 UTC.~~ The covered region at  
4 18 UTC is 20° - 55°N and 85° - 155°W, which includes the western USA and sea area near the  
5 west coast (Figure 1).

6 The experiment design includes six simulations (Table 1). The control (CTRL) experiment  
7 is first made with an initial time at 18:00 UTC ~~of~~from 30 June to 30 July and makes 6-h forecasts.  
8 The five data assimilation (DA) experiments and the continued ~~second~~-control experiment are  
9 made with initial time at 00:00 UTC from July 1 to 31, 2012 and make a 72-h forecast for each  
10 day. The initial condition in all six experiments is obtained from the 6-h forecasts of the first  
11 control experiment. The five DA experiments are made with different data sets including  
12 conventional data ~~only~~-(CON), microwave data (AMSU-A + MHS) ~~only~~-(MW), infrared data  
13 (IASI) ~~only~~-(IR), a combination of microwave and infrared data (MWIR), a combination of  
14 conventional, microwave and infrared observation data (ALL). The initial condition and lateral  
15 boundary conditions came from the operational GFS forecast at 6-h intervals and 0.5 x 0.5  
16 degree resolution, which were downloaded from NCEP data inventory  
17 (<ftp://ftp.ncep.noaa.gov/pub/data/nccf/com/gfs/prod/>).

18 In the ARW model, the physics of the model includes the Goddard Cumulus Ensemble  
19 (GCE) microphysics scheme, Yonsei University planetary boundary layer (PBL) scheme, Noah  
20 land surface model, Rapid Radiative Transfer Model (RRTM) longwave radiation, and the  
21 Goddard shortwave radiation scheme ([Xu et al., 2009](#)). The 15-km WRF model forecast with a  
22 mesh size domain of 718 X 373 (Fig.1) was used. Forty-three (43) vertical layers were selected  
23 for use with a model top of 10 hPa.

### 1 3. Data and Methodology

#### 2 3.1 Conventional and Satellite data

3 In this study, the conventional observation data includes atmospheric temperature (T),  
4 moisture (Q) and wind speed (WSP) at various pressure levels and pressure data at the surface  
5 [that were downloaded from NCEP data inventory \(ftp://ftp.ncep.noaa.gov/pub/data/  
6 nccf/com/gfs/prod/\)](ftp://ftp.ncep.noaa.gov/pub/data/nccf/com/gfs/prod/). Figure 1a shows the distribution of the conventional data on July 1, 2012  
7 where the atmospheric temperature, moisture and surface pressure observations are rare. Most of  
8 atmospheric temperature and moisture observations are conducted at the surface level in [the](#)  
9 pressure range of 1000-1200 hPa. ~~Most of the~~ [The most](#) WSP data are found over the sea close to  
10 the [western](#) coast of ~~western-the~~ United States.

11 The satellite data includes the Advanced Microwave Sounding Unit-A (AMSU-A),  
12 Microwave Humidity Sounder (MHS) and the new generation Infrared Atmospheric Sounding  
13 Interferometer (IASI). Figure 1b shows the distribution of the AMSU-A, MHS and IASI datasets  
14 [acquired about at 18:00 UTC on July 1, 2012](#). AMSU-A is a 15-channel cross-track, stepped-line  
15 scanning, total power microwave radiometer. ~~In this study the~~ channels from 4 to 14 are  
16 assimilated ~~in this study~~, which were designed to detect atmospheric temperature at 11 layers  
17 from the surface to around 45 km. Their weighting function is illustrated ~~in by~~ Figure 2a. MHS  
18 on the other hand probes at millimetric frequencies between 89 and 183 GHz, the channels from  
19 2 to 5 are assimilated, which were designed to detect atmospheric moisture at 2 layers from  
20 surface to around 400 hPa. Their weighting function is illustrated ~~in by~~ Figure 2b. Channel 4 of  
21 AMSU-A and channel 2 of MHS can detect the atmospheric temperature and humidity at the  
22 lowest layer of the troposphere. Channels 5 and 6 of AMSU-A and channels 3, 4 and 5 of MHS  
23 can ~~represent~~ [detect](#) the atmospheric temperature and humidity in the middle atmospheric layer of

1 | the troposphere. Channel 7 of AMSU-A can ~~indicate~~ detect the atmospheric temperature in the  
2 | highest layer of troposphere. Channels 9 and 10 of AMSU-A can detect the atmospheric  
3 | temperature in lower layer of the stratosphere

4 | The IASI instrument covers the spectral range from the thermal infrared at 3.62  $\mu\text{m}$  (2760  
5 |  $\text{cm}^{-1}$ ) to 15.5  $\mu\text{m}$  (645  $\text{cm}^{-1}$ ) covering the peak of the thermal infrared and particularly the CO<sub>2</sub>  
6 | band with the humidity (Q) branch around 666  $\text{cm}^{-1}$ . Within these bands, the selected 279 bands  
7 | (Table 2) correspond to atmospheric temperature and humidity. A band number smaller than  
8 | 515 represents atmospheric temperature, and a band number larger than 2701 represents  
9 | atmospheric humidity. Their weighting function is illustrated ~~in~~ by Figure 2c.

### 10 | 3.2 Radiance data quality control and bias correction

11 | The radiance data have been preprocessed by [NOAA's Satellite and Information Service](#)  
12 | [\(NESDIS\)](#) before becoming available for usage. The data have been statistically limb corrected  
13 | (adjusted to nadir) and surface emissivity corrected in the microwave channels and cloud cleared  
14 | in the tropospheric channels. Although the satellite data have undergone preprocessing, they  
15 | need further bias correction before being ingested into data assimilation system. The source of  
16 | the biases can be related to instrument calibration problems, and predictor and zenith angle bias.  
17 | It was demonstrated that a successful bias correction scheme must take into account the spatially  
18 | varying and air-mass dependent nature of radiance biases. ~~Previous publications have~~ (Kelly and  
19 | Flobert, 1988; McMillin et al., 1989; Uddstrom, 1991). Eyre (1992) and Harris and Kelly  
20 | (2001) categorized the bias into two types: scan bias and air-mass bias, and presented a bias  
21 | correction scheme. GSI uses this bias correction scheme to correct radiance bias. The radiance  
22 | bias correction coefficients ~~might~~ ~~may~~ be downloaded from [Global Data Assimilation System](#)  
23 | [\(GDAS\)](#) ~~(define GDAS)~~ data directory (<ftp://ftp.ncep.noaa.gov/pub/data/nccf/com/gfs/prod/>).

1 and it can be used to correct the radiance bias in GSI. To that purpose in this study, monthly  
 2 regional mean innovations, e.g. observation minus background (OMB) and observation minus  
 3 analysis (OMA), are calculated with or without bias corrections in this study. For example, Fig.  
 4 ~~ure-3 is shows~~ the scattering plots of surface pressure (Fig. 3a), atmospheric temperature at the  
 5 height of 2m (Fig. 3b)~~2-meters~~ and wind speed at the height of 10m (Fig. 3c)~~10-meters~~ between  
 6 OMB and OMA in the ALL data experiment. The result shows that the slope of the simulated  
 7 line is less than 1, which indicates the analysis fields are closer to observation than background  
 8 fields.

### 9 3.3 Methodology

10 In order to evaluate the effects of radiance data assimilation on temperature and moisture  
 11 at the different vertical layers, the surface (SFC) and four atmospheric layers are examined. The  
 12 four layers include lower troposphere (LT) from 800 to 1000 hPa, middle troposphere (MT) from  
 13 400 to 800 hPa, upper troposphere (UT) from 200 to 400 hPa and lower stratosphere (LS) from  
 14 50 to 200 hPa. Similar to ~~the a~~ previous study (Xu, et al., 2009), two statistical variables - bias  
 15 and root mean square (RMS) errors s are investigated.

16 If X represents any of the parameters under consideration for a given time and vertical level,  
 17 then the forecast error is defined as  $X' = X_f - X_o$  where the subscripts *f* and *o* denote forecast and  
 18 observed quantities, respectively. Given N valid pairs of forecasts and observations, the bias is  
 19 computed as

$$20 \quad bias = \overline{X'} = \frac{1}{N} \sum_{i=1}^N X'_i \quad (1)$$

21 the root mean-square (RMS) error is computed as

$$22 \quad RMS = \sqrt{\frac{1}{N} \sum_{i=1}^N (X'_i)^2} \quad (2)$$

1 The bias and RMS error at 00:00 and 12:00 UTC are calculated because more than enough  
2 observational data and approximately 3000 sounding stations can be used at the two times.

## 3 4. Results

### 4 4.1 Impact of DA on Temperature

5 At the SFC, the CON (conventional data only) DA experiment shows (Fig.4a) the smallest  
6 bias value in all six experiments. ~~The three involved~~ infrared satellite DA experiments  
7 (IR, IR+MW, IR+MW+CON) ~~showing~~ a larger bias than the CTRL experiment. ~~For the first 24~~  
8 ~~hours,~~ it seems that satellite radiance DA, especially for the infrared IASI data, make a negative  
9 contribution to the temperature forecasts. ~~Interestingly~~~~In additon,~~ the bias characterized a  
10 diurnal cycle feature for the 72-h forecasts, with the smaller bias appearing at 06, 30, 54 and 72-h  
11 corresponding to a local time at 4:00 pm while the higher bias appeared at 18, 42 and 66-h  
12 corresponding to 4:00 am local time.

13 Compared to the SFC, the LT shows a more clear diurnal variation (Fig. 4b), and all model  
14 forecasts underestimated the observed temperature. The CTRL and CON experiments obtained  
15 the smallest forecast bias.

16 Different from the SFC and LT, the diurnal variation of bias disappeared in the MT (Fig.  
17 4c). Compared to the CTRL experiment, the bias is significantly reduced in all DA experiments  
18 especially for the two combination experiment (MWRI and ALL), the bias is almost zero ~~with~~~~in~~  
19 the 30-h forecast. It implies that both MW (AMUS-A and MHS) and IR (IASI) DA ~~make~~~~give~~ a  
20 positive contribution to the accuracy of temperature forecasts at the MT.

21 At the UT, the smaller bias appeared ~~at~~~~in~~ the CON and MW DA experiments (Fig. 4d), and  
22 the combination DA experiments (MWIR and ALL) show a larger bias than the CTRL  
23 experiment. The results indicate that the IR DA ~~made~~ a negative contribution to the

1 temperature forecasts and the MW experiment improved the forecast accuracy in the UT.

2 | In contrast, the bias in the LS indicates an opposite pattern to the SFC and LT ~~that~~ where  
3 all satellite DA experiments reduced the forecast bias (Fig. 4e). The result demonstrated that the  
4 | conventional DA did not improve the forecasts because of the sp~~r~~arse observational data used in  
5 this layer. The MW DA obtained the smallest bias ~~at~~ in the LS.

6 | In order to clearly understand the different performance in the six experiments, the  
7 temperature forecast bias profile at 6-h, 30-h and 54-h has been examined. Fig. 5 indicates a  
8 similar pattern at the three forecast times where the lower bias can be found at the SFC and MT  
9 while the larger bias appeared at the UT and LS. Generally, the model forecasts overestimated  
10 the observed temperature except in the LT. Compared to the CTRL experiment, the four satellite  
11 DA experiments (MW, IR, MWIR and ALL) show a smaller bias from the MT through LS, but  
12 the forecasts did not get improved in the LT below 800 hPa. In contrast, the CON experiment has  
13 better performance in the LT, especially at the SFC.

14 | It is obvious that the larger bias in temperature forecast appeared in the LT, UT and LS, but  
15 the model is underestimating the observed temperature in the LT and overestimating in the UT  
16 and LS (Fig. 5). The satellite DA, especially for the MW DA experiment using AMSU-A,  
17 | reduced the forecast bias at the levels from the MT to LS. Meanwhile, the CON DA has a  
18 smaller forecast bias in the LT, especially at the SFC. Note the IR experiment using the IASI  
19 data produced a worst result in the LT.

20 | The forecast RMS error demonstrated some different features (Fig. 6). First, the RMS error  
21 | reduced the diurnal variation and ~~the RMS error~~ it significantly increased with the extended  
22 length of forecast time at the SFC. The RMS error in the CON and MW experiments is slightly  
23 less than that in the CTRL experiment and the other three satellite DA experiments within 24-h

1 forecasts (Fig. 6a). Second, consistent with the larger negative bias in all the satellite DA  
2 experiments (Fig. 4b) in the LT, larger RMS errors are observed in these DA experiments (Fig.  
3 6b) compared to the CTRL. Third, different from the smaller bias in the DA experiments, the  
4 larger RMS errors are maintained in the DA experiments in the MT (Fig. 6c). Fourth, the CON  
5 and MW experiments improved the temperature forecasts in the UT (Fig. 6d). But in the LS, the  
6 ~~involved~~ microwave DA experiments including MW, MWIR and ALL indicate ~~the~~ smaller RMS  
7 errors than the CTRL experiments (Fig. 6e). It is apparent that the CON DA ~~made-gave~~ a  
8 negative contribution to the temperature forecast in the LS.

9 Corresponding to the bias profile (Fig. 5), the forecast RMS error profile at 6-h, 30-h and  
10 54-h indicates (Fig. 7) that the smallest RMS error is observed at the MT and the largest RMS  
11 error appeared in the LT and SFC. Compared to the CTRL experiment, the smaller RMS errors  
12 are only found in the MW experiment in the UT and LS, and the CON DA made a positive  
13 contribution at the SFC and UT.

14 The results clearly show the IR DA experiment ~~makes-gives~~ a negative contribution to the  
15 temperature forecast in the regional system. But the MW DA experiment shows a positive  
16 ~~impacted contribution~~ at the LS, and the CON experiment displays better performance at the SFC  
17 and UT. It is worth noticing that the RMS error is not always consistent with the bias in the  
18 temperature forecasts, for example, the smaller bias appeared at the SFC while a larger RMS  
19 error is observed there.

## 20 **4.2 Impact of DA on hHumidity**

21 Similar to the temperature forecasts at the SFC, the diurnal variation of the moisture bias is  
22 observed and the smallest bias appeared in the CON and CTRL experiments within the 42-h  
23 forecast (Fig. 8a) with largest bias occurring in the MWIR experiment at 18-h. It is clear that all

1 four satellite DA experiments do not improve the moisture forecast compared to the CTRL  
2 experiment. In contrast, the IR DA produced a larger bias significantly differ~~ent~~<sup>ing</sup> from the  
3 other experiments in the entire troposphere (Fig. 8b,c,d). It seems to tell us that the IR DA  
4 significantly impacts the humidity forecasts in the troposphere. However, the impacts  
5 disappeared in the LS (Fig. 8e).

6 Compared to the bias profile of the temperature forecast (Fig 4), all model runs  
7 overestimated the observed humidity except for the UT. The smallest bias in the humidity  
8 forecast occurred at the SFC and UT (Fig. 9). Most of DA experiments apparently reduced the  
9 bias from LT to UT, especially for the IR experiment. But it is worth noting that the MW DA  
10 has a larger bias than the CTRL experiment in the whole troposphere.

11 However, the RMS error in the humidity forecasts (Fig. 10) increases from the SFC to LS.  
12 The largest error in the UT and LS is almost double the amount at the SFC. In addition, most of  
13 DA experiments demonstrated a larger RMS error than that in the CTRL experiment. In other  
14 words, the DA experiments ~~made-gave~~ a negative contribution to the humidity forecasts. The IR  
15 DA experiment did not improve moisture forecast although its bias is very small at the LT and  
16 MT.

## 17 **5. Summary and Discussion**

### 18 **5.1 Summary**

19 In this study, six experiments were designed to assess the effects of data assimilation on  
20 atmospheric temperature and moisture forecasts over the western United States. The results are  
21 summarized as follows.

22 The regional model underestimates the observed temperature in the LT and overestimates  
23 it in the UT and LS. The MW experiment reduced the forecast bias from the MT to LS, and the



1 CON DA obtained a smaller forecast bias in the LT, especially at the SFC. But the IR  
2 experiment using the IASI data obtained the largest bias in the LT.

3 However, the RMS error is not always consistent with the bias profile in the temperature  
4 forecasts. ~~in fact,~~ the RMS error profile shows that the largest RMS error appeared in the LT  
5 and the smallest error in the MT. Compared to the CTRL experiment, the smaller RMS errors are  
6 only found in the MW experiment in the UT and LS, and the CON DA ~~made-gave~~ a positive  
7 contribution at the SFC and in the UT. The IASI DA experiment ~~hasmade~~ a negative  
8 ~~impacted contribution onto~~ the temperature forecast in the regional forecast system.

9 In contrast, all model forecasts overestimated the observed humidity except in the UT. The  
10 smallest bias in the humidity forecast occurred at the SFC and in the UT. Most of DA  
11 experiments apparently reduced the bias in the LT to UT, especially for the IR DA experiment.  
12 But the MW DA obtained a larger bias than the CTRL experiment in the entire troposphere.

13 The RMS error in the humidity forecasts increases from the SFC to the LS, which is similar  
14 to the bias profile except in the UT. The largest error in the UT and LS is almost double the  
15 amount at the SFC. The DA experiments ~~make-give~~ a limited contribution to the humidity  
16 forecasts. The IR DA experiment does not improve the moisture forecast although its smallest  
17 bias is found in the LT and MT.

## 18 5.2 Discussion

19 This is a study using WRF-ARW mesoscale model ~~linked to linkage with~~ GSI data  
20 assimilation system to explore the impacts of AMSU-A/MHS and IASI radiance data  
21 assimilation on the temperature and humidity forecasts in the different vertical layers over the  
22 western coast of United States, due to the complexity of measurements for satellite instruments  
23 (such as IASI has 8461 channels) and lack of knowledge in the estimation of impacts of those

1 | datasets in this regional area, forecasters should be aware of the limitations of these data  
2 | assimilation when forecasting in this region.

3 |         The results show that the bias and forecast error is substantially related to the vertical  
4 | layer of the objective. For example, the AMSU-A data assimilation reduced the temperature  
5 | forecast bias in the upper atmospheric layers, the conventional data assimilation indicates the  
6 | best performance in the lower layer, but the IASI data assimilation shows worst performance in  
7 | the lower layer. Compared to the largest bias in the upper atmospheric layer, the largest RMS  
8 | error appeared in the lower atmospheric layers. ~~For the~~ The humidity forecast ~~there is a~~ different  
9 | ~~behavior~~; the IASI data assimilation significantly reduced the bias in the troposphere, but the  
10 | RMS error tells us that the IASI data assimilation does not improve the moisture forecast in this  
11 | layer. The reason is very complicated, it is partially attributed to the data selection in the  
12 | processes of the data assimilation. The results ~~showed~~ in this analysis demonstrate the  
13 | ~~partial~~ ~~some~~ impacts of satellite data on temperature and humidity forecasts in this region, but the  
14 | positive or negative impact depends on the atmospheric layer and forecasts variables.

15 |         It is worth noting that the results presented here are based on one month's forecasts with  
16 | three satellite instruments. The model performance needs to be examined with longer  
17 | experiments and more data selection that extend to all available satellite data sets and more  
18 | experiments from the different areas. As expressed by Manning and Davis (1997), "These  
19 | statistics would provide additional information to model users and alert model developers to  
20 | those research areas that need more attention."

#### 21 | ***Acknowledgements.***

22 | The GSI data assimilation system was obtained from Joint Center for Satellite Data Assimilation  
23 | (JCSDA), WRF-ARW model was obtained from the NCAR, the satellite datasets were provided

1 by NOAA/NESDIS/STAR. The authors would like to thank these agencies for the model and  
2 data providing. This work was partially supported by a project funded by the Priority Academic  
3 Program Development of Jiangsu Higher Education Institutions (PAPD), the National Natural  
4 Science Foundation of China (No. 40701130), the No-for-Profit Industry (Meteorology)  
5 Research Program, China (GYHY201106027), and Jiangsu Key Laboratory of Meteorological  
6 Observation and Information Processing (S5311026001) at the Nanjing University of  
7 Information Science and Technology, Nanjing, China.

8 This work was partially supported by the National Oceanic and Atmospheric Administration  
9 (NOAA), National Environmental Satellite, Data, and Information Service (NESDIS), Center for  
10 Satellite Applications and Research (STAR). The views, opinions, and findings contained in this  
11 publication are those of the authors and should not be considered an official NOAA or U.S.  
12 Government position, policy, or decision.

### 13 **Reference**

14 Andersson, E., A. Hollingsworth, G. Kelly, P. Lönnberg, J. Pailleux, and Z. Zhang, 1991: Global  
15 observing system experiments on operational statistical retrievals of satellite sounding  
16 data. *Mon. Wea. Rev.*, **119**, 1851–1864.

17 Clerbaux C., A. Boynard , L. Clarisse , M. George , J. Hadji-Lazaro , H. Herbin , D. Hurtmans ,  
18 M. Pommier, A. Razavi , S. Turquety, C. Wespes and P.-F. Coheur, 2009: Monitoring  
19 of atmospheric composition using the thermal infrared IASI/MetOp sounder. *Atmos.*  
20 *Chem. Phys.*, 9, 6041– 6054, 2009. [www.atmos-chem-phys.net/9/6041/2009/](http://www.atmos-chem-phys.net/9/6041/2009/)

21 Collard AD. 2007. Selection of IASI channels for use in numerical weather prediction. *Q. J. R.*  
22 *Meteorol. Soc.* **133**: 1977–1991

23 Derber J. C. and W-S Wu. 1998: The use of TOVS cloud-cleared radiances in the NCEP SSI

1 analysis system. *Mon. Wea. Rev.*, **126**, 2287–2299.

2 Eyre J. A bias correction scheme for simulated TOVS brightness temperatures. Tech. Memo.  
3 186, ECMWF (1992).

4 Han Y., Paul van Delst, Q. Liu, F. Weng, B. Yan, R. Treadon and J. Derber, 2006: JCSDA  
5 Community Radiative Transfer Model (CRTM) - Version 1, *NOAA Tech Report 122*.

6 Harris B. and Kelly G., A satellite radiance bias correction scheme for data assimilation *Quart. J.*  
7 *Roy. Meteorol. Soc.* 127, 1453 (2001).

8 Kelly GA, Flobert JF. 1988. Radiance tuning. In: *Technical Proceedings of the Fourth*  
9 *International TOVS Study Conference*, Igls, Austria, 16–22 March 1988: 99–117.

10 Liu Q, Weng F. Detecting the warm core of a hurricane from the Special Sensor Microwave  
11 Imager Sounder. *Geophys. Res. Lett.* 2006; 33: L06817, doi:10.1029/2005GL025246.

12 Liu, Q., and F. Weng, 2006: Advanced doubling–adding method for radiative transfer in  
13 planetary atmosphere. *J. Atmos. Sci.*, **63**, 3459–3465.

14 Liu, Zhiqian, Craig S. Schwartz, Chris Snyder, and So-Young Ha. "Impact of assimilating  
15 AMSU-A radiances on forecasts of 2008 Atlantic tropical cyclones initialized with a  
16 limited-area ensemble Kalman filter", *Monthly Weather Review*, 2012.

17 Manning, K. W., and C. A. Davis, 1997: Verification and sensitivity experiments for the  
18 WISP95 MM5 forecasts. *Weather Forecasting*, **12**, 719–735

19 McMillin, L. M., L. J. Crone, and D. S. Crosby, 1989: Adjusting satellite radiances by regression  
20 with an orthogonal transformation to a prior estimate. *J. Appl. Meteor.*, 28, 969–975.

21 McNally, A. P., J. C. Derber, W. Wu, and B. B. Katz, 2000: The use of TOVS level-1b radiances  
22 in the NCEP SSI analysis system. *Quart. J. Roy. Meteor. Soc.*, **126**, 689–724.

23 Moncet, J., G. Uymin, and H. E. Snell, 2004: Atmospheric radiance modeling using the Optimal

1 Spectral Sampling (OSS) method. Preprints, *SPIE Defense and Security Symp., Conf.*  
2 *5425: Algorithms and Technologies for Multispectral, Hyperspectral, and Ultraspectral*  
3 *Imagery X*, Orlando, FL, Society of Photo-Optical Instrumentation Engineers, 5425–  
4 5437.

5 Nutter, P. A., and J. Manobianco, 1999: Evaluation of the 29-km Eta Model. Part I: Objective  
6 verification at three selected stations. *Wea. Forecasting*, 14, 5–17.

7 Parrish DF, Derber JC (1992) The National Meteorological Center's spectral statistical  
8 interpolation analysis system. *Mon Wea Rev* 20:1747–1763

9 Rabier F, Fourri e N, Chafa i D, Prunet P. 2002. Channel selection methods for Infrared  
10 Atmospheric Sounding Interferometer radiances. *Q. J. R. Meteorol. Soc.* **128**: 1011–1027.

11 Rodgers CD. 1996. 'Information content and optimisation of high spectral resolution  
12 measurements'. pp 136–147 in: *Optical Spectroscopic Techniques and Instrumentation*  
13 *for Atmospheric and Space Research II*, SPIE 2380, Hays PB, Wang J (eds).

14 Rodgers CD. 2000. *Inverse Methods for Atmospheres: Theory and Practice*. World Scientific:  
15 Singapore.

16 Uddstrom, M., 1991: Forward model errors. Proc. 6th Int. TOVS Study Conference, Airlie,  
17 Virginia, Cooperative Institute for Meteorological Satellite Studies, Space Science and  
18 Engineering Center, University of Wisconsin, USA, 501–516.

19 Wan, Q. and J Xu, 2011: A numerical study of the rainstorm characteristics of the June 2005  
20 flash flood with WRF/GSI data assimilation system over south-east China. *Hydrological*  
21 *Processes*, **25**, 1327–1341 (2011) DOI: 10.1002/hyp.7882

22 Weng F., 2007: Advances in Radiative Transfer Modeling in Support of Satellite Data  
23 Assimilation. *J. Atmos. Sci.*, **64**, 3799–3807

1 Xu J., S. Rugg, L. Byerle, and Z. Liu, 2009: Weather Forecasts by the WRF-ARW Model with  
 2 the GSI Data Assimilation System in the Complex Terrain Areas of Southwest Asia.  
 3 *Wea. Forecasting*, **24**, 987–1008.

4 Xu, J and A Powell, 2011: Dynamical Downscaling Precipitation over the Southwest Asian:  
 5 Impacts of Radiance Data Assimilation on the Hindcasts of the WRF-ARW Model,  
 6 *Atmospheric Research*. doi:10.1016/j.atmosres.2012.03.005

7 Zapotocny, T. H., Jung, J. A., Le Marshall, J. F. and Treadon, R. E. 2008: A Two Season Impact  
 8 Study of Four Satellite Data Types and Rawinsonde Data in the NCEP Global Data  
 9 Assimilation System. *Wea. Forecast.*,23, 80 – 100.

10 Zhou, H., G´omez-Herna´ndez, J. J., Hendricks Franssen, H.-J., Li, L., 2011. An approach to  
 11 handling nongaussianity of parameters and state variables in ensemble kalman filtering.  
 12 *Advances in Water Resources*.34 (7), 844–864, DOI: 10.1016/j.advwatres.2011.04.014.

13  
14  
15

16 **Table 1** The experiment design includes six simulations (EXP1-EXP6)

	<b>Experiment</b>	<b>Description</b>	<b>Initial time</b>
<b>EXP1</b>	CTRL	Control experiment without data assimilation	<u>18 UTC from 30 June to 31 July</u>
<b>EXP2</b>	CON	Conventional data assimilation	<u>00 UTC from 1 to 31 July</u>
<b>EXP3</b>	MW	AMSU-A+MHS data assimilation	<u>00 UTC from 1 to 31 July</u>
<b>EXP4</b>	IR	IASI data assimilation	<u>00 UTC from 1 to 31 July</u>
<b>EXP5</b>	MWIR (MW+IR)	AMSU-A+MHS+IASI data assimilation	<u>00 UTC from 1 to 31 July</u>
<b>EXP6</b>	ALL	Conventional+AMSU-A+MHS+IASI	<u>00 UTC from 1 to 31 July</u>

Formatted Table

	(CON+MW+IR)	data assimilation	
--	-------------	-------------------	--

1  
2  
3  
4  
5  
6  
7

8 **Table2** Listed below are the 279 Channels in IASI corresponding to atmospheric temperature  
9 and humidity. The numbers indicate the order in which the channels were chosen in current data  
10 assimilation

16	135	226	356	566	1658	2993	3248	3509	5502
38	138	230	360	571	1671	3002	3252	3518	5507
49	141	232	366	573	1786	3008	3256	3527	5509
51	144	236	371	646	1805	3014	3263	3555	5517
55	146	239	373	662	1884	3027	3281	3575	5558
57	148	243	375	668	1991	3029	3303	3577	5988
59	151	246	377	756	2019	3036	3309	3580	5992
61	154	249	379	867	2094	3047	3312	3582	5994
63	157	252	381	906	2119	3049	3322	3586	6003
66	159	254	383	921	2213	3053	3375	3589	
70	161	260	386	1027	2239	3058	3378	3599	
72	163	262	389	1046	2271	3064	3411	3653	
74	167	265	398	1121	2321	3069	3438	3658	
79	170	267	401	1133	2398	3087	3440	3661	
81	173	269	404	1191	2701	3093	3442	4032	
83	176	275	407	1194	2741	3098	3444	5368	
85	180	282	410	1271	2819	3105	3446	5371	
87	185	294	414	1479	2889	3107	3448	5379	
104	187	296	416	1509	2907	3110	3450	5381	
106	193	299	426	1513	2910	3127	3452	5383	
109	199	303	428	1521	2919	3136	3454	5397	

111	205	306	432	1536	2939	3151	3458	5399
113	207	323	434	1574	2944	3160	3467	5401
116	210	327	439	1579	2948	3165	3476	5403
119	212	329	445	1585	2951	3168	3484	5405
122	214	335	457	1587	2958	3175	3491	5455
125	217	345	515	1626	2977	3178	3497	5480
128	219	347	546	1639	2985	3207	3499	5483
131	222	350	552	1643	2988	3228	3504	5485
133	224	354	559	1652	2991	3244	3506	5492

1  
2  
3  
4  
5

6 **Caption of Figures**

7 **Fig. 1** Distribution of observations. (a) conventional data on July 1, 2012 with the atmospheric  
8 temperature (yellow), moisture (dark blue) and surface pressure(light blue ), wind speed  
9 (orange). (b) Scan coverage of AMSU-A (light blue), MHS (dark blue) and IASI (red)  
10 radiance at 18:00 UTC on July 1, 2012

11 **Fig. 2** Vertical weighting functions for satellite observations as a function of height. (a)  
12 AMSUA , (b) MHS , (c) IASI

13 **Fig. 3** The scattering plot between observation minus background [OMB] and observation minus  
14 analysis [OMA] in the all data ( Conventional+AMSU-A+MHS+IASI ) experiement  
15 (a: surface pressure, b: atmospheric temperature at the height of 2 meters,  
16 c: wind speed at the height of 10 meters) for 1 July 2012

17 **Fig. 4** Bias of the temperature (T) forecasts at (a) surface (SFC), (b) lower troposphere (LT),



1 (c) middle troposphere (MT), (d) upper troposphere (UT), (e) lower stratosphere (LS).

2 Unit: °C. CTRL , CON , MW, IR, MWIR and ALL are defined in Table 1

3 **Fig. 5** Bias profile of the temperature (T) forecasts at (a) 6-h , (b) 30-h, (c) 54-h forecasts.

4 | Unit: °C. ~~Other definitions are the same of Fig. 4. The other definition is same as Fig. 4.~~

5 **Fig. 6** RMSE of the temperature (T) forecasts at (a) surface (SFC), (b) lower troposphere (LT),

6 (c) middle troposphere (MT), (d) upper troposphere , (e) lower stratosphere. Unit: °C

7 | ~~Other definitions can be found in Table 1. The other definition can be found Table 1.~~

8 **Fig. 7** The RMSE profile of the temperature forecasts at (a) 6-h , (b) 30-h, (c) 54-h forecasts.

9 | Unit: °C. ~~Other definitions are the same of Fig. 4. The other definition is same as Fig. 4.~~

10

11 **Fig. 8** The bias of the specific humidity (Q) forecasts at (a) surface (SFC), (b) lower troposphere

12 (LT), (c) middle troposphere (MT), (d) upper troposphere , (e) lower stratosphere. Unit:

13 | g/kg. ~~Other definitions can be found in Table 1. The other definition can be found~~

14 ~~Table 1.~~

15 **Fig. 9** Bias profile of the specific humidity forecasts at (a) 6-h , (b) 30-h, (c) 54-h forecasts.

16 | Unit: g/kg. ~~Other definitions are the same of Fig. 4. The other definition is same as Fig. 4.~~

17 **Fig. 10** The RMSE profile of the specific humidity forecasts at (a) 6-h , (b) 30-h, (c) 54-h

18 | forecasts. Unit: g/kg. ~~Other definitions are the same of Fig. 4. The other definition is~~

19 ~~same as Fig. 4.~~

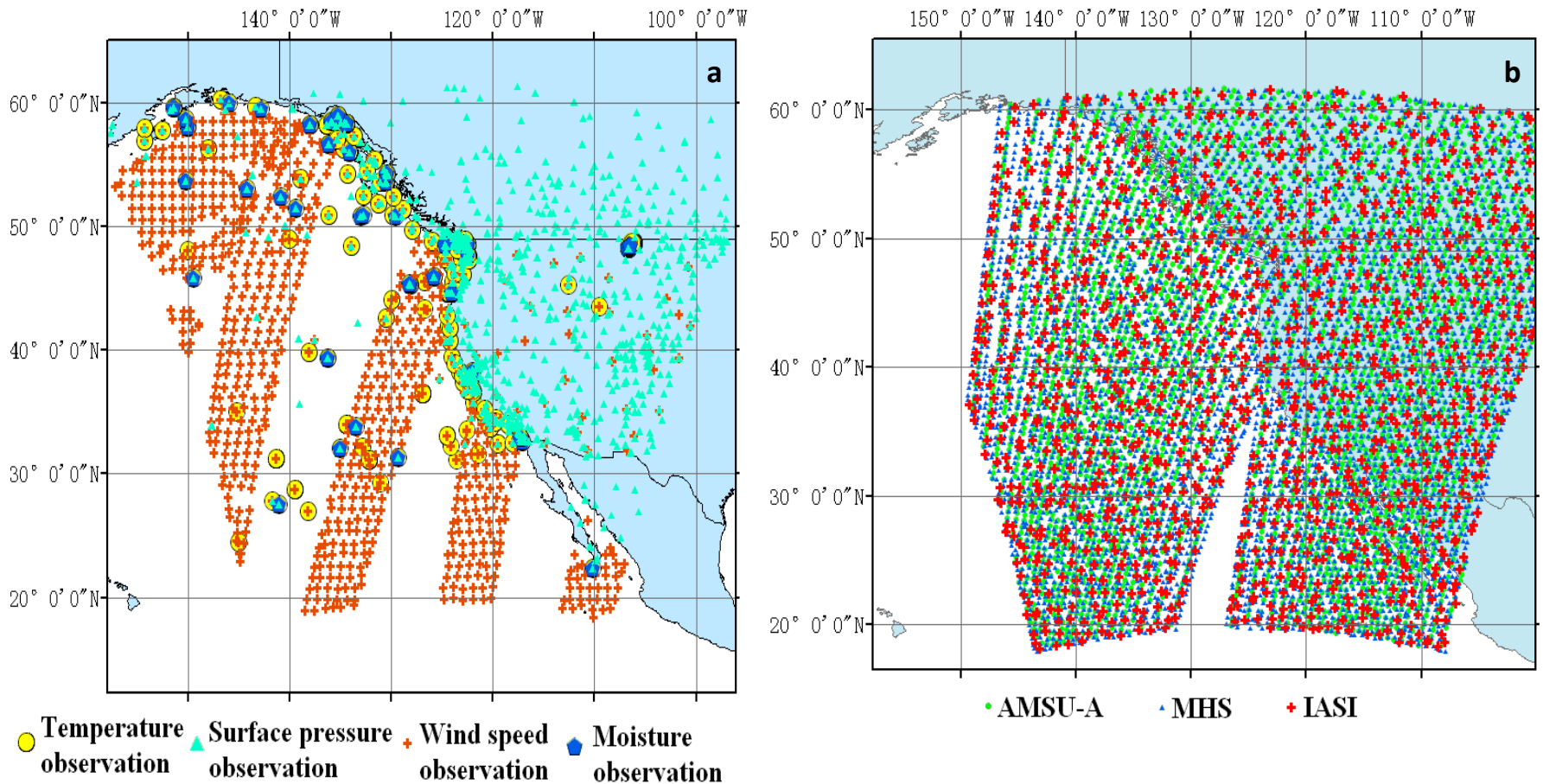


**Fig. 1** Distribution of observations. (a) conventional data on July 1, 2012 with the atmospheric temperature (yellow), moisture (dark blue) and surface pressure (light blue), wind speed (orange). (b) Scan coverage of AMSU-A (light blue), MHS (dark blue) and IASI (red) radiance at 18:00 UTC on July 1, 2012

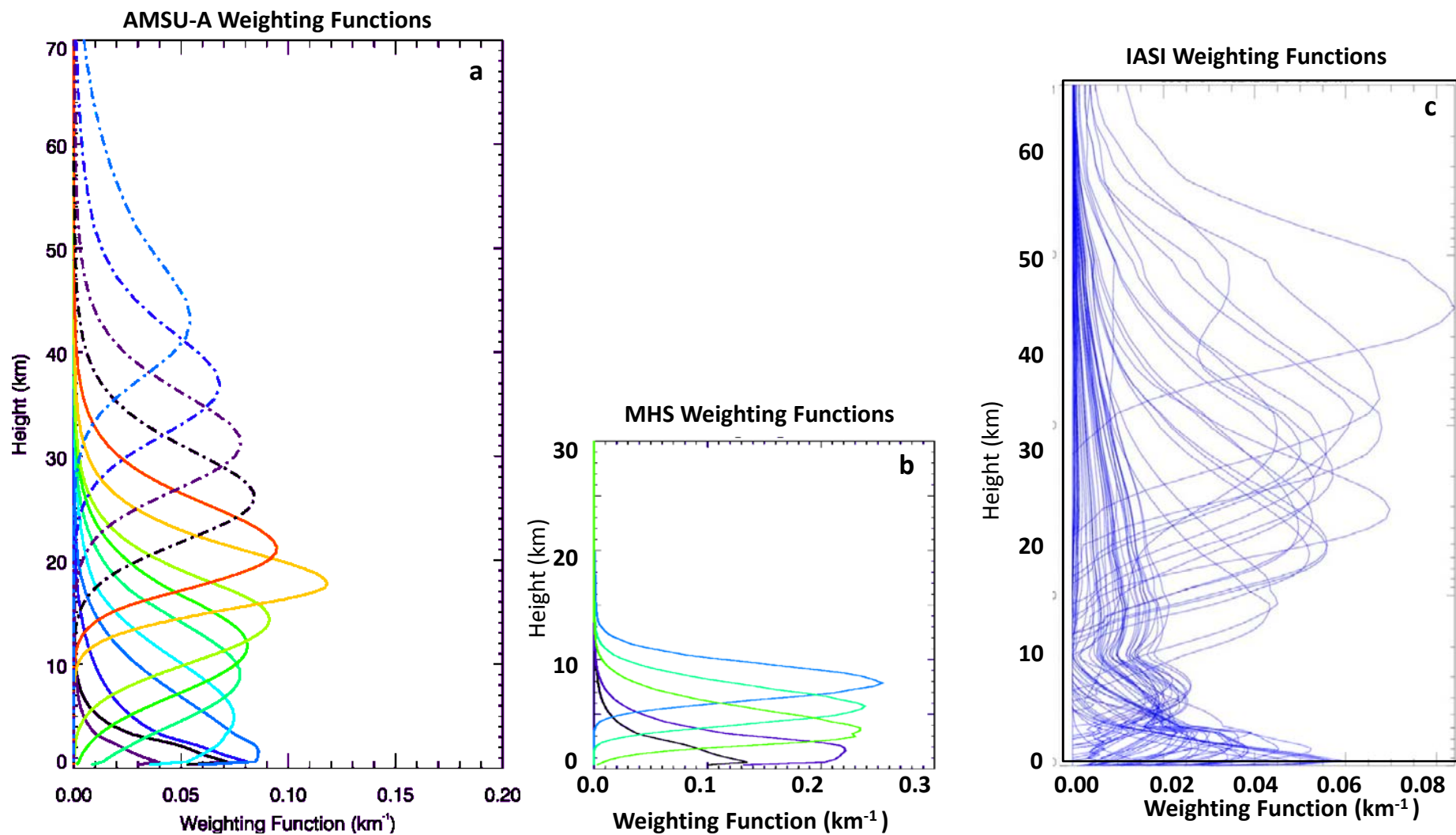


**Fig. 2** Vertical weighting functions for satellite observations as a function of height. (a) AMSUA , (b) MHS , (c) IASI

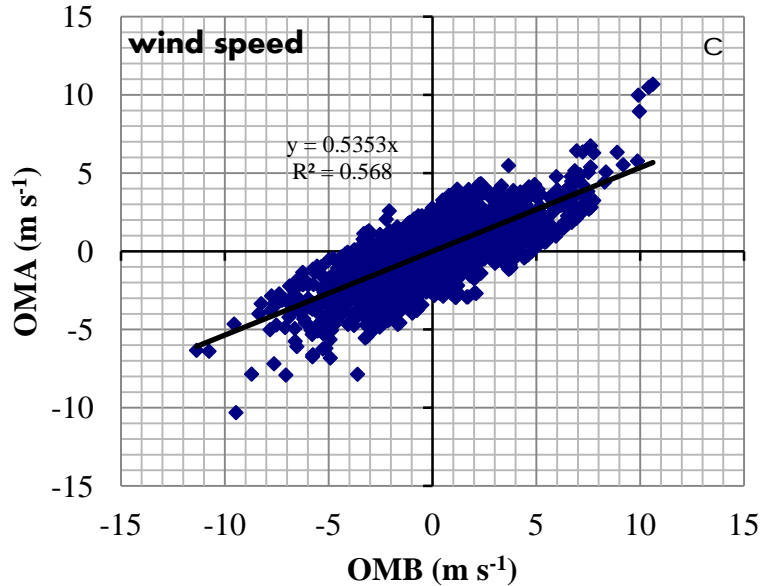
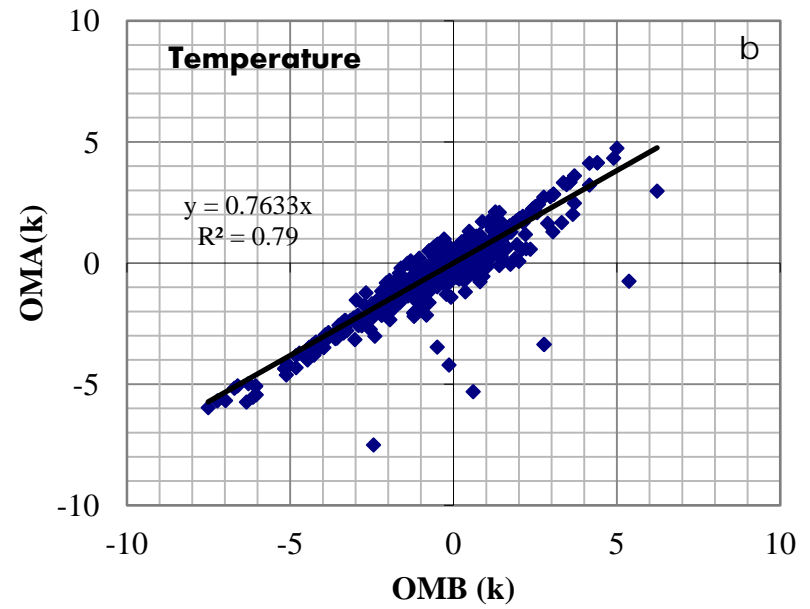
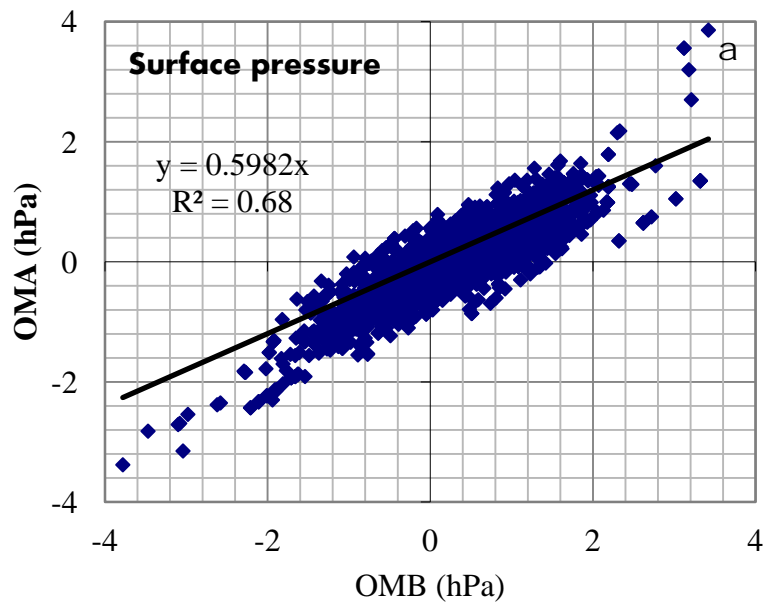


**Fig. 3** The scattering plot between observation minus background [OMB] and observation minus analysis [OMA] in the all data ( Conventional+AMSU-A+MHS+IASI ) **experiment** (a: surface pressure, b: atmospheric temperature at the height of 2 meters, c: wind speed at the height of 10 meters) for 1 July 2012

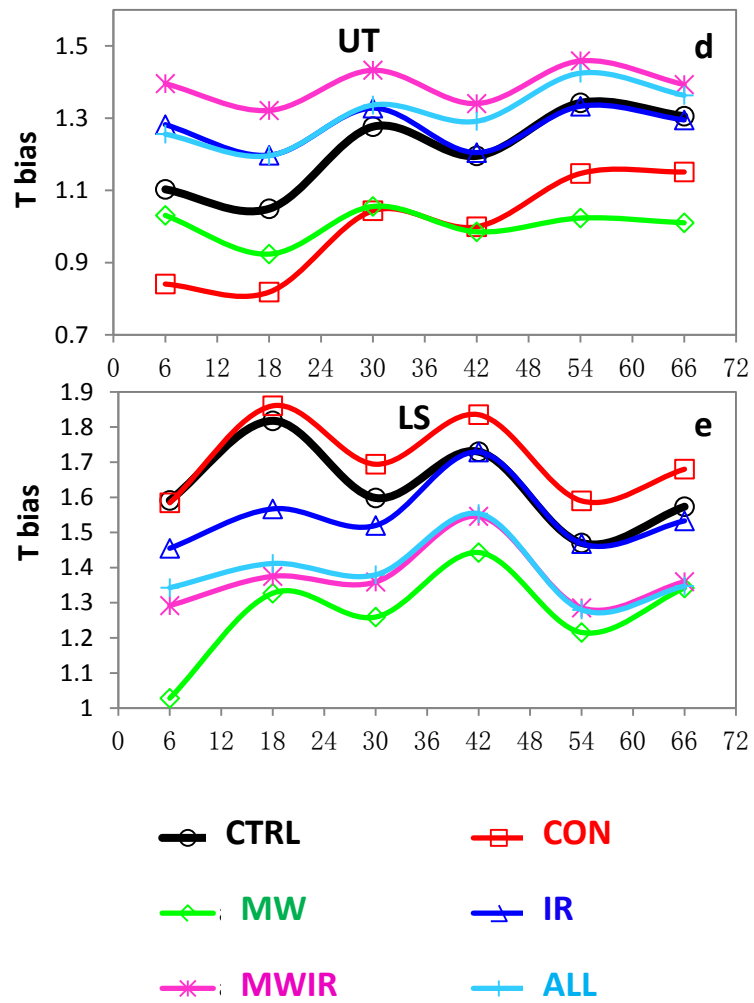
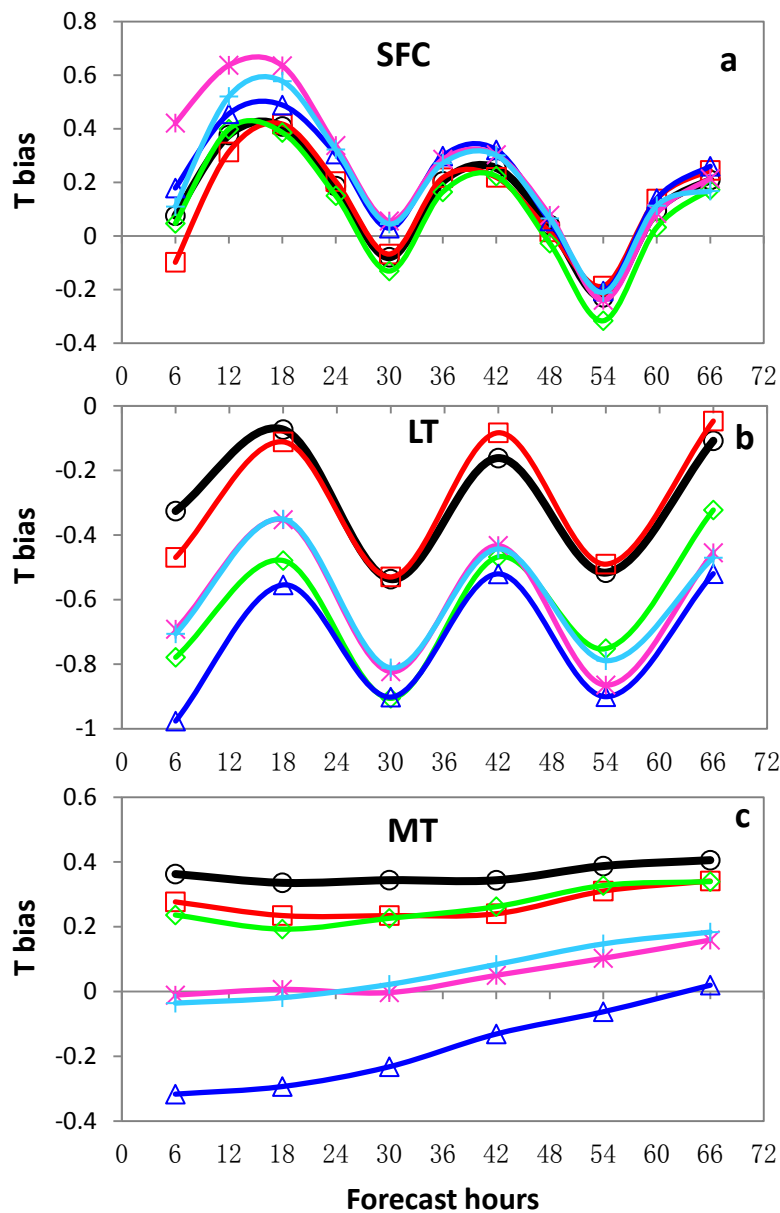


**Fig. 4** Bias of the temperature (T) forecasts at (a) surface (SFC), (b) lower troposphere (LT), (c) middle troposphere (MT), (d) upper troposphere (UT), (e) lower stratosphere (LS). Unit: °C. CTRL, CON, MW, IR, MWIR and ALL are defined in Table 1

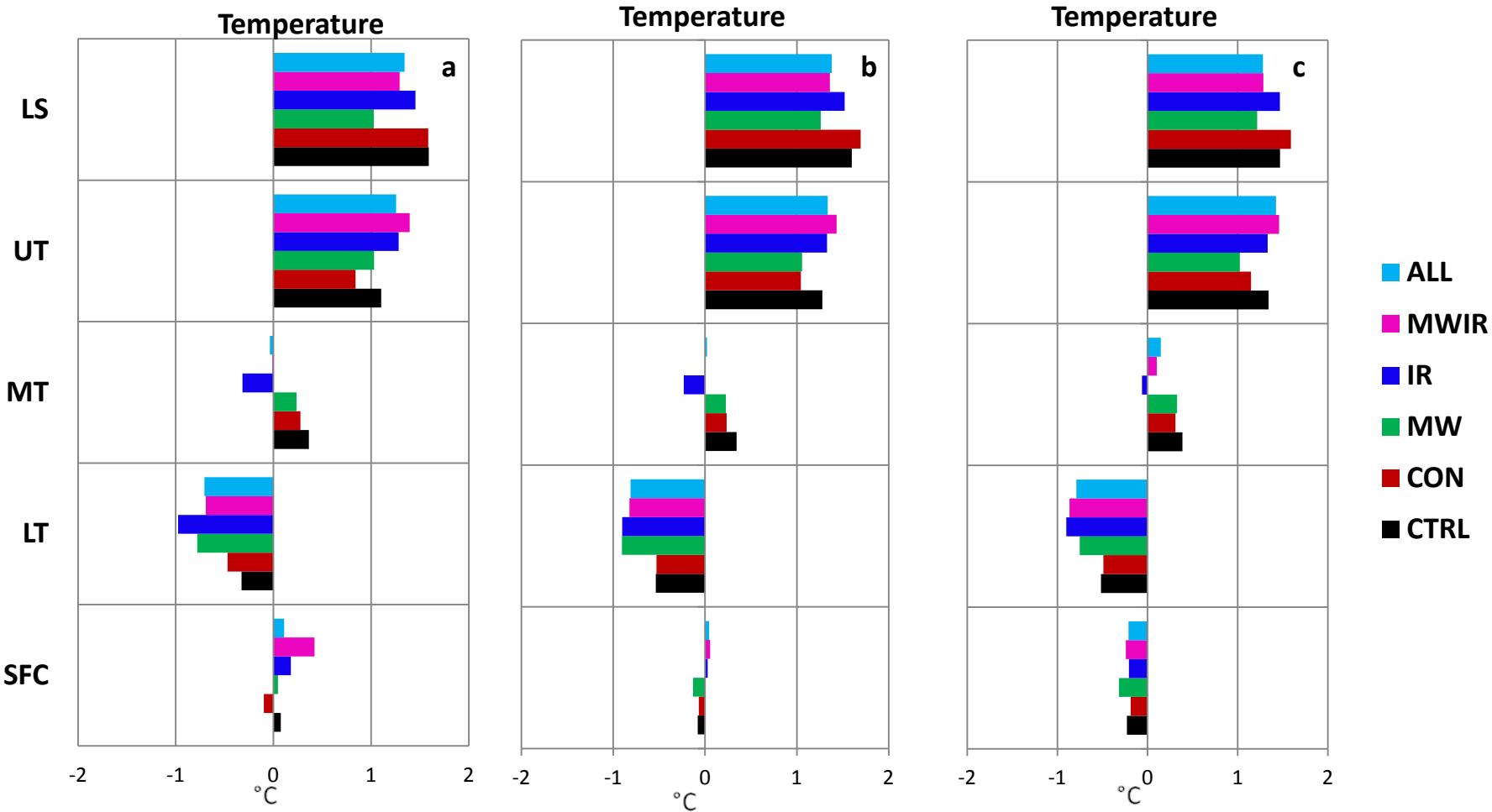


**Fig. 5** Bias profile of the temperature (T) forecasts at (a) 6-h , (b) 30-h, (c) 54-h forecasts. Unit:  $^{\circ}\text{C}$ . Other definitions are the same of Fig. 4.

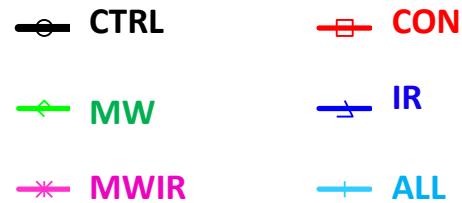
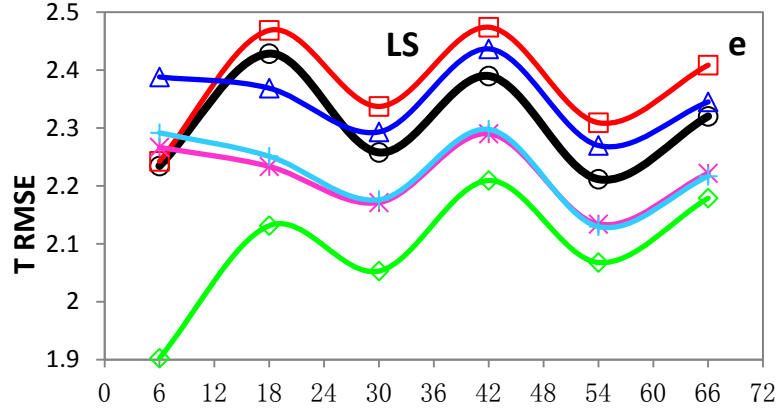
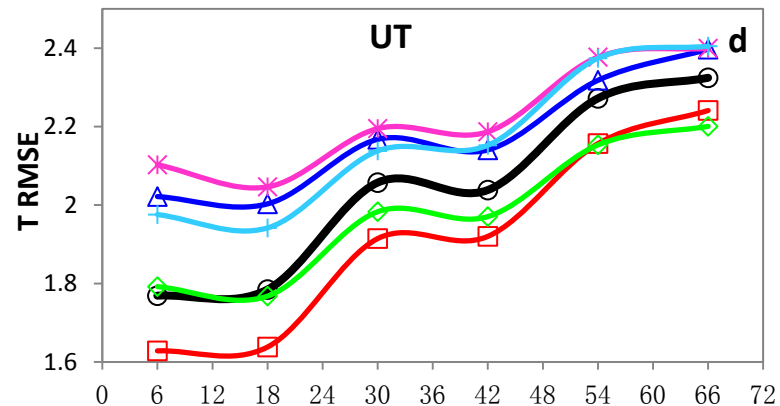
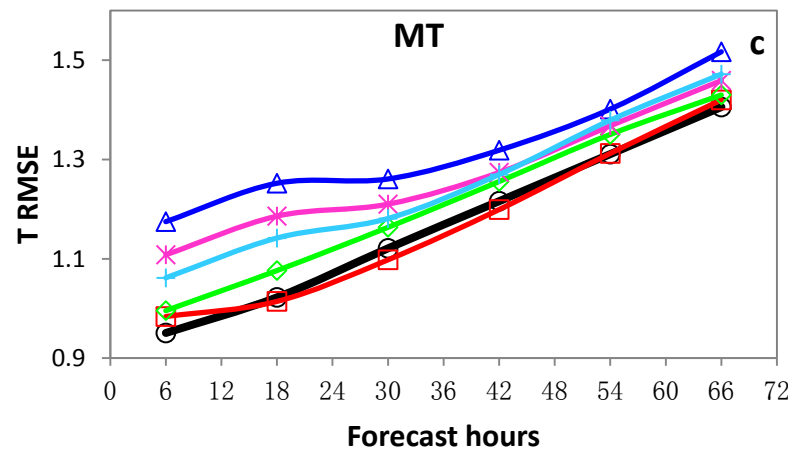
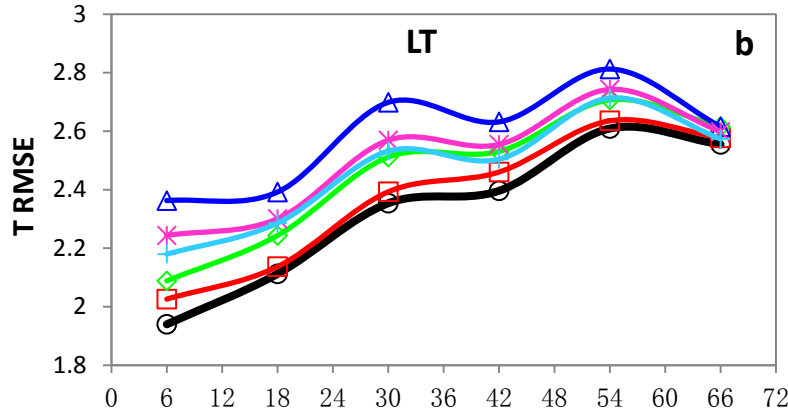
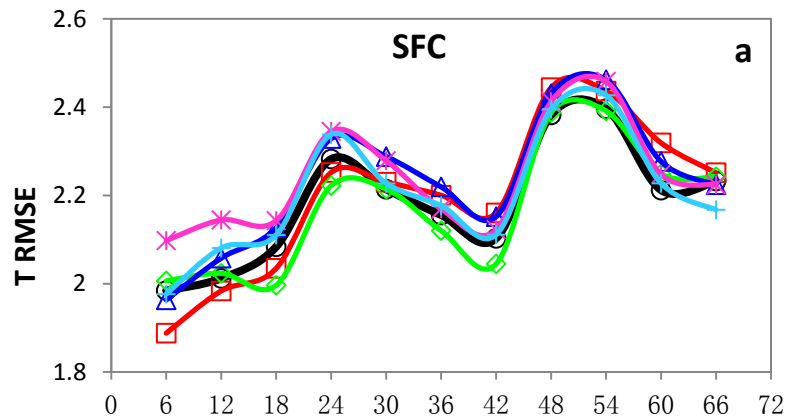


**Fig. 6** RMSE of the temperature (T) forecasts at (a) surface (SFC), (b) lower troposphere (LT), (c) middle troposphere (MT), (d) upper troposphere, (e) lower stratosphere. Unit: °C. Other definitions can be found in Table 1.

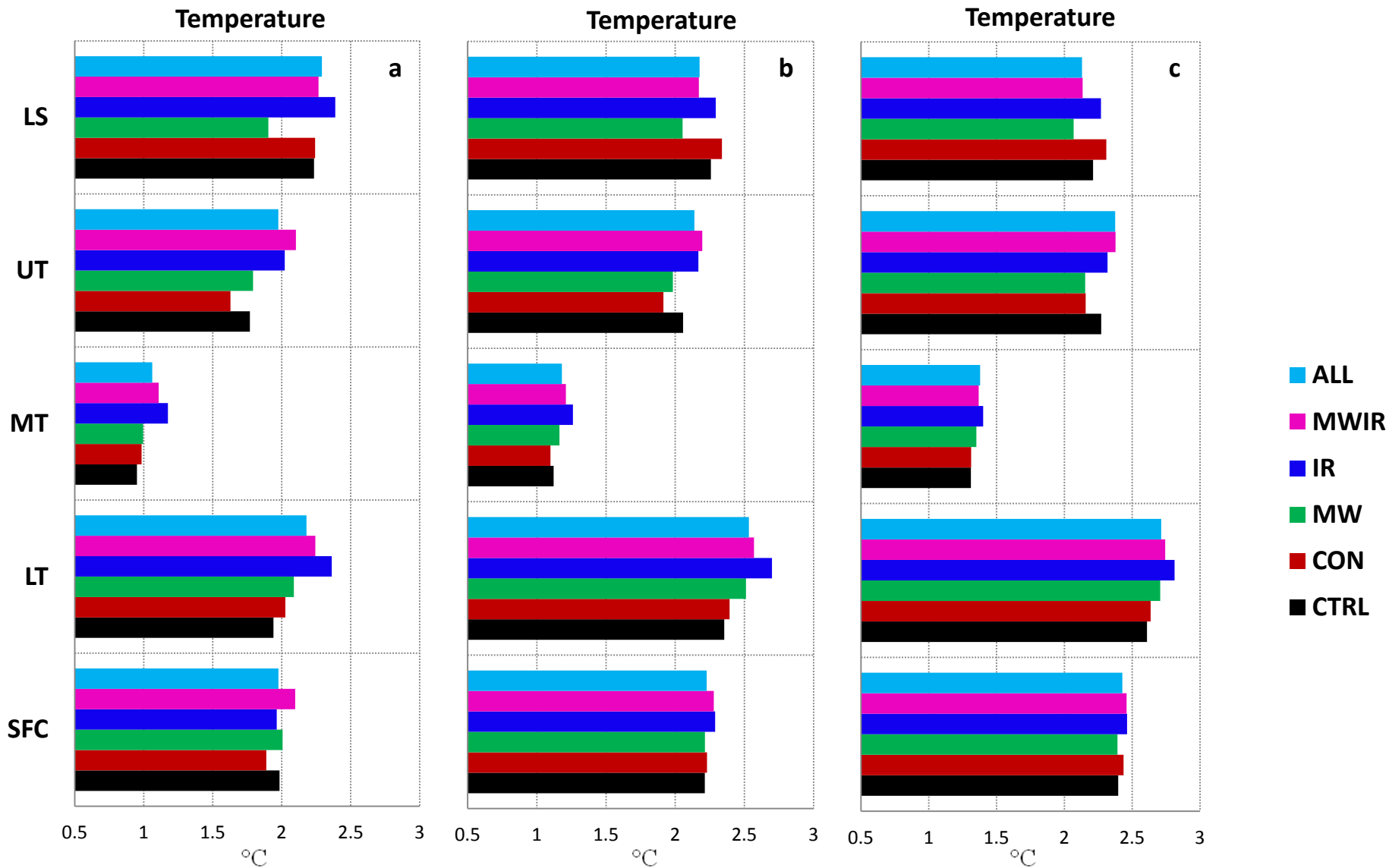


**Fig. 7** The RMSE profile of the temperature forecasts at (a) 6-h , (b) 30-h, (c) 54-h forecasts. Unit: °C. Other definitions are the same of Fig. 4.



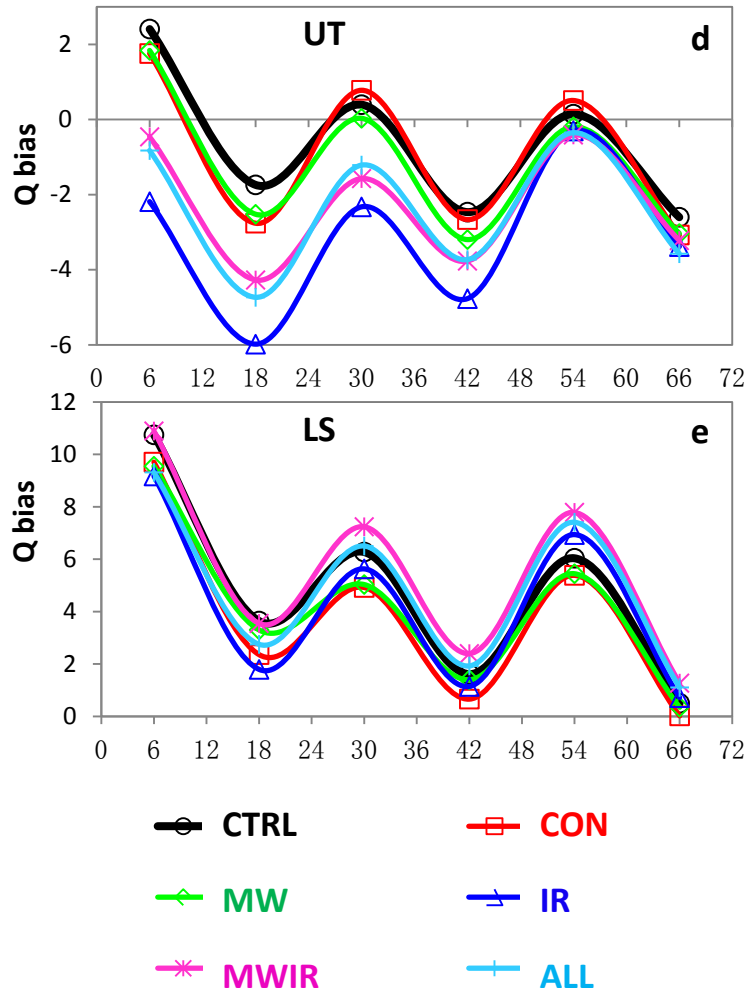
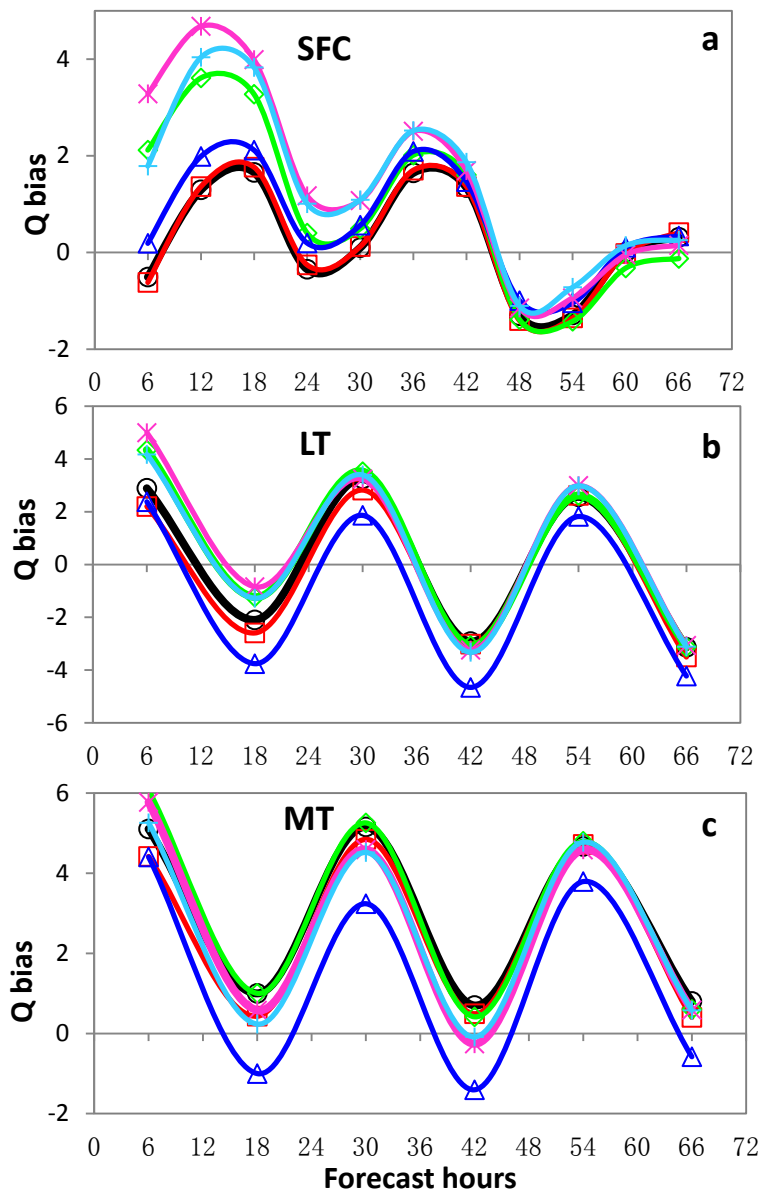


**Fig. 8** The bias of the specific humidity (Q) forecasts at (a) surface (SFC), (b) lower troposphere (LT), (c) middle troposphere (MT), (d) upper troposphere, (e) lower stratosphere. Unit: g/kg. Other definitions can be found in Table 1.

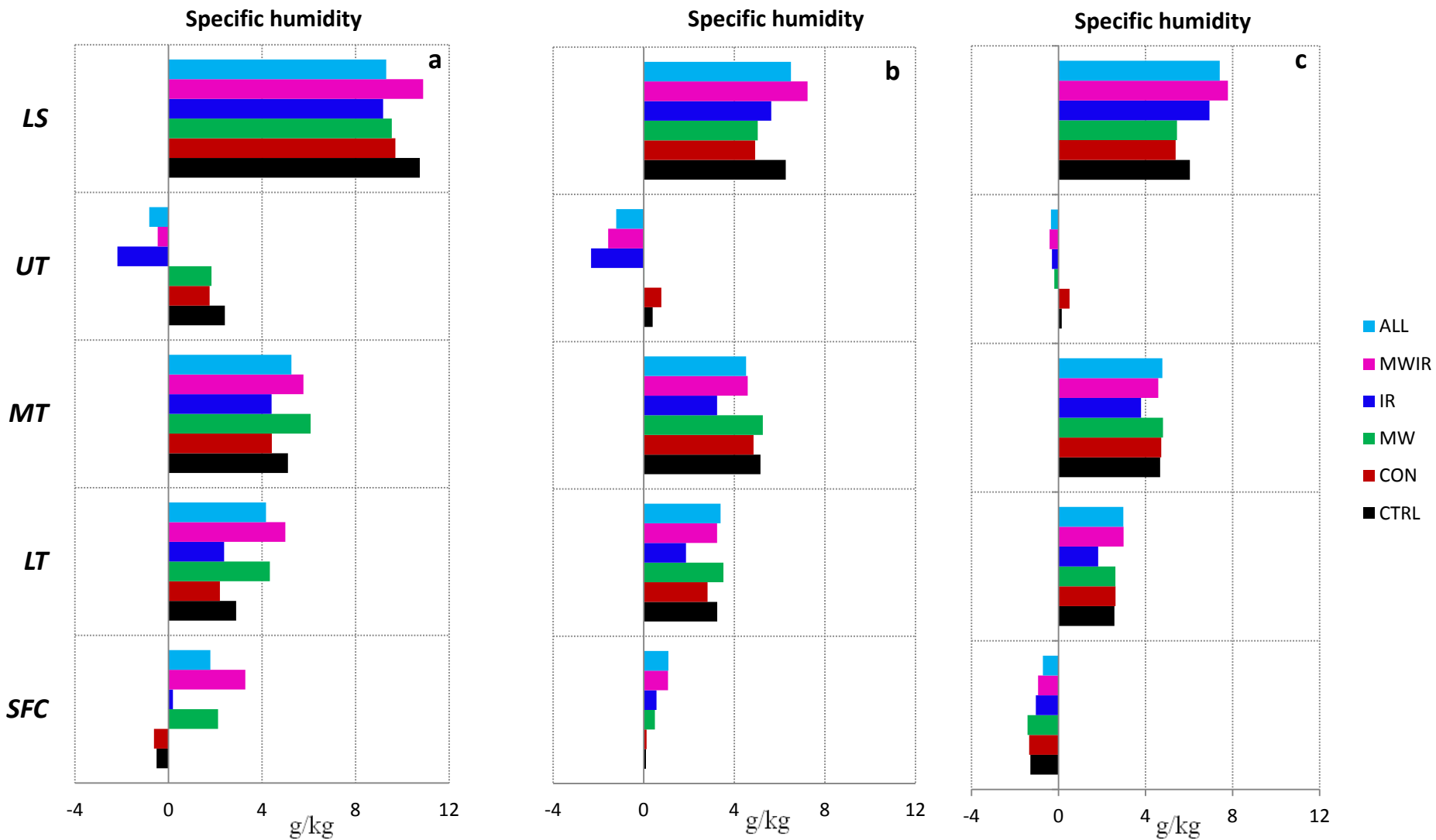


**Fig. 9** Bias profile of the specific humidity forecasts at (a) 6-h , (b) 30-h, (c) 54-h forecasts. Unit: g/kg. Other definitions are the same of Fig. 4.

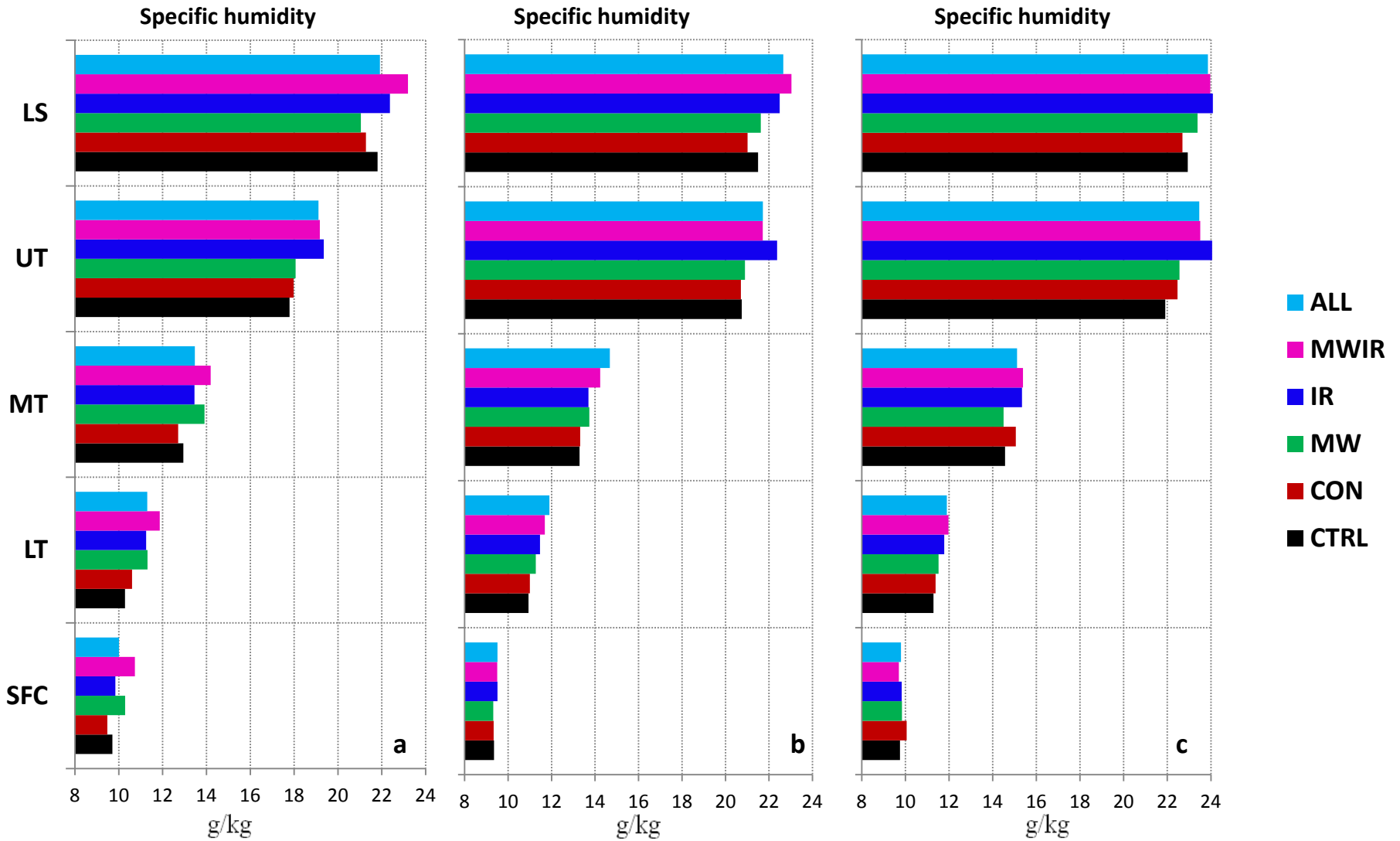


**Fig. 10** The RMSE profile of the specific humidity forecasts at (a) 6-h , (b) 30-h, (c) 54-h forecasts. Unit: g/kg. Other definitions are the same of Fig. 4.